Supplemental Information for:

Vector-free DNA transfection by nuclear envelope mechanoporation

Leyla Akh,[a,1] Apresio K. Fajrial,[b,1] Sunwoo Sohn[b], Benjamin Seelbinder,[b] Xin Xu,[b] Wei Tan,[ab] Jill Slansky,[c] Corey P. Neu,[abd] Xiaoyun Ding.[abd]*

[a] *Biomedical Engineering Program, University of Colorado, Boulder, CO 80309, USA.*
[b] *Paul M. Rady Department of Mechanical Engineering, University of Colorado, Boulder, CO 80309, USA.*
[c] *University of Colorado School of Medicine, CO 80309, USA.*
[d] *BioFrontiers Institute, University of Colorado, Boulder, CO 80309, USA.*

* Corresponding author: Xiaoyun Ding
Email: xiaoyun.ding@colorado.edu

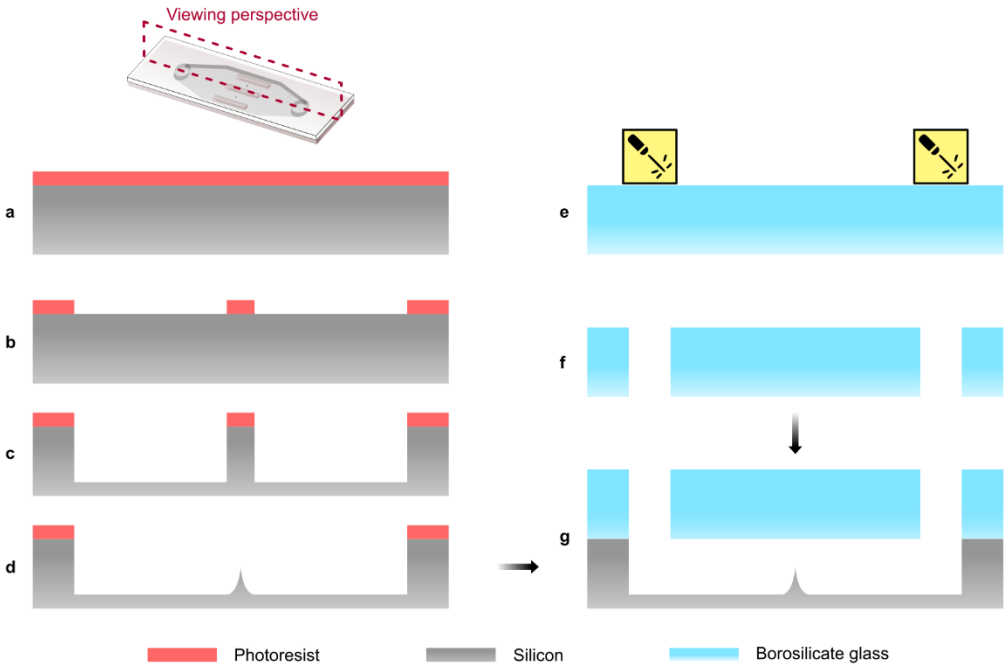

Supplementary Figure 1 | Fabrication process workflow of the NEST device. a-d, Fabrication of sharp tip nanostructure in microchannel on silicon substrate consists of photolithography, deep reactive ion etching, and isotropic etching from a combination of oxide growth and BOE. **e-f**, Inlet and outlet holes fabrication using laser engraver on a borosilicate glass substrate. **g**, Anodic bonding of the silicon and glass substrate with aligned inlet/outlet position.

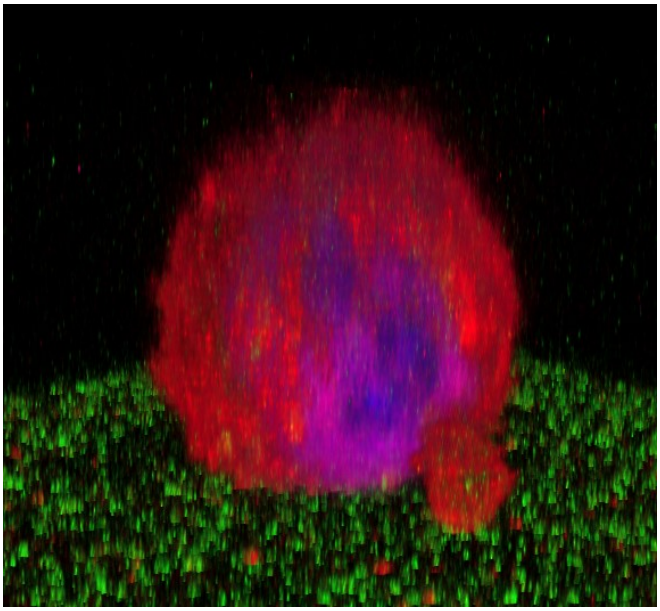

Supplementary Figure 2| Confocal micrograph of a NEST-treated cell. A 3D reconstruction of a confocal micrograph showing a HeLa cell after NEST treatment, revealing a pore in both the cell membrane and the nuclear envelope. The plasma membrane of the cell is red, the nuclear envelope is magenta, and the nuclear contents are blue.

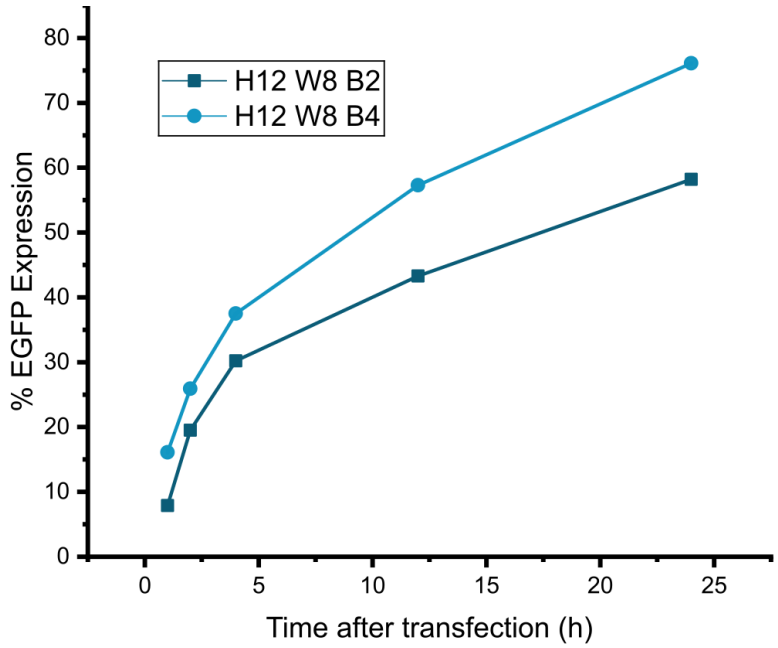

Supplementary figure 3 | Device dimensions affecting transfection efficiency. HeLa cells were transfected using NEST device of the indicated dimensions, where H indicates the height of the channel in microns, W is the width of the channel in microns, and B is the blade length in microns. The device with a blade length of 4um showed superior transfection of EGFP-encoding plasmid DNA.

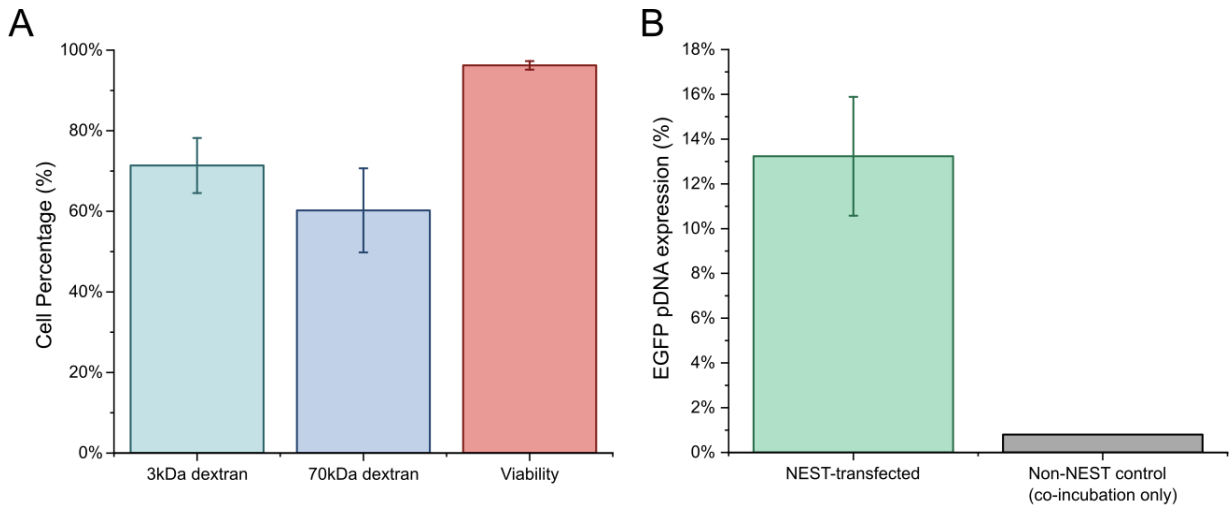

Supplementary Figure 4 | NEST delivery and transfection in C2C12 mouse myoblasts. (A) Delivery of 3kDa and 70kDa dextrans to C2C12 cells. (B) NEST transfection efficiency of naked EGFP-encoding plasmid DNA into C2C12 cells.

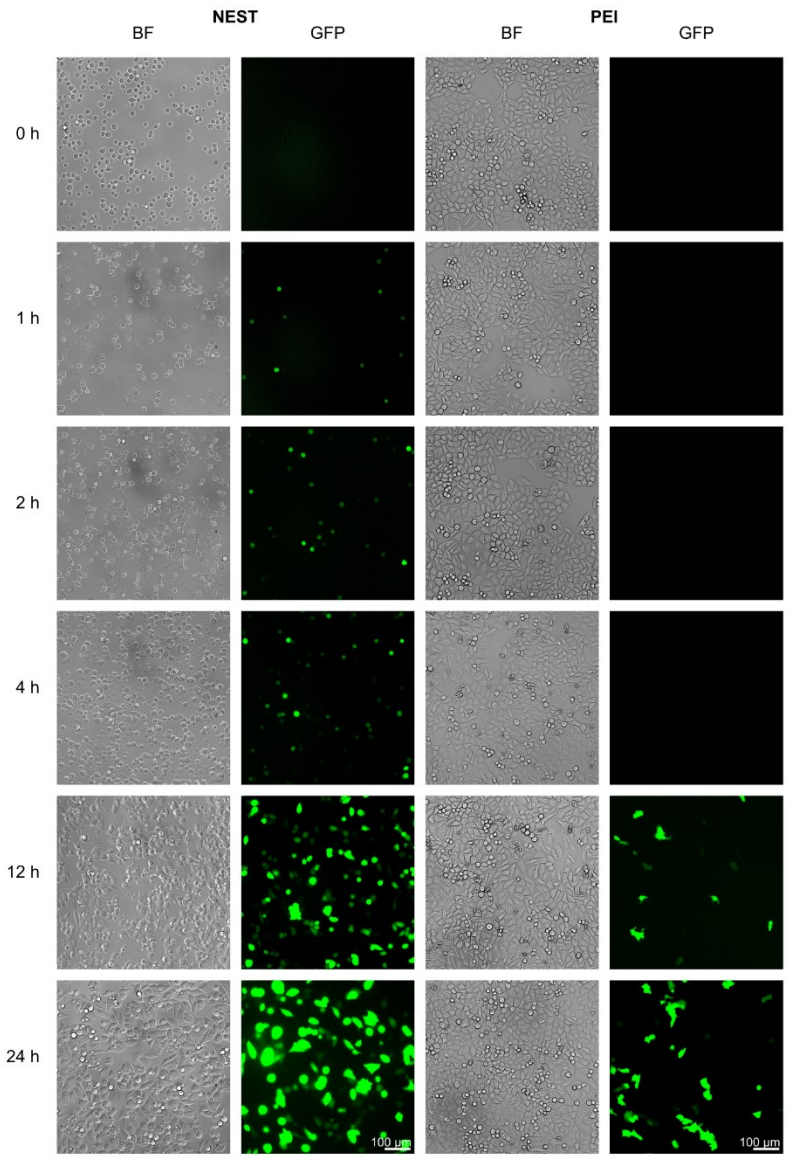

Supplementary Figure 5 | Fluorescence microscopy images of EGFP transfected cells using NEST and PEI methods. The images were recorded at time points 0, 1, 2, 4, 12, and 24 hours as shown in the figure.

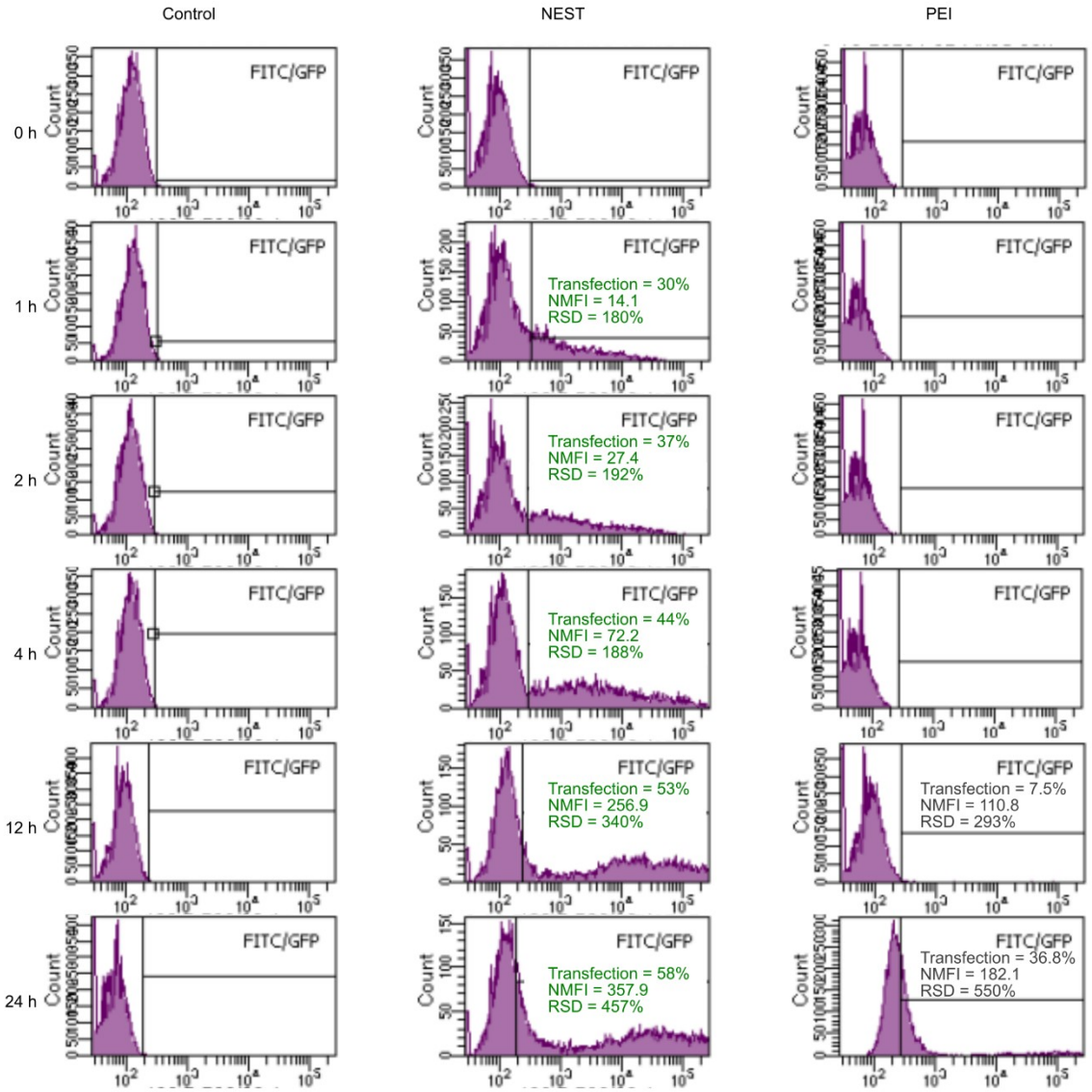

Supplementary Figure 6 | Transfection efficiency assessment of the various intracellular delivery methods using flow cytometry. The expression of plasmid DNA at time points 0, 1, 2, 4, 12, and 24 h is shown in the figure.

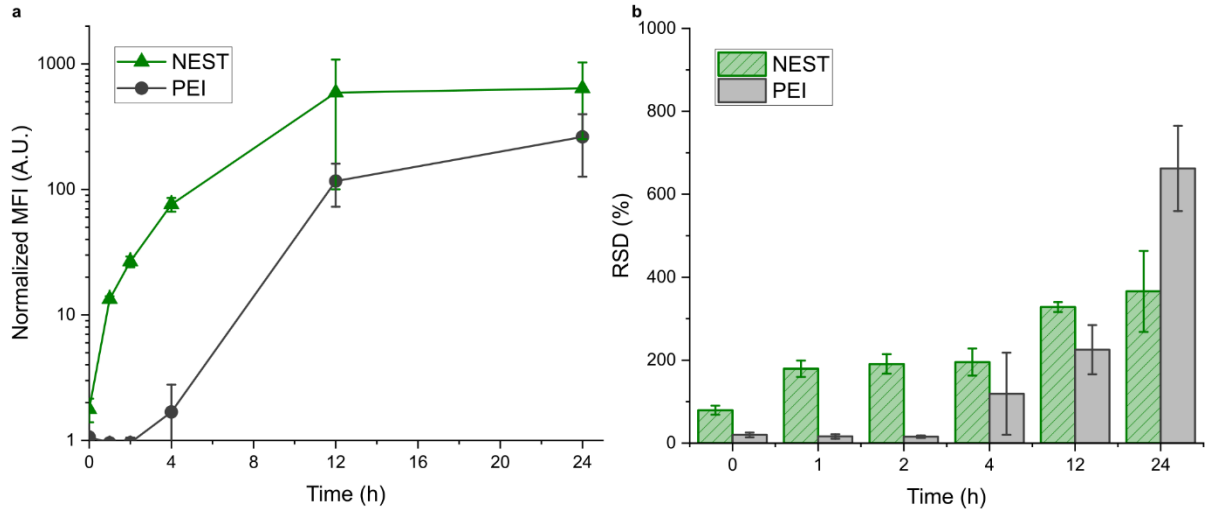

Supplementary Figure 7 | Quantitative assessment of flow cytometry data from EGFP transfected cells using NEST and PEI methods at time points 0, 1, 2, 4, 12, and 24 hours. a, Normalized Mean Fluorescence Intensity (MFI) **b,** Relative Standard Deviation (RSD)**.** Error bars represent s.d. (n = 3)

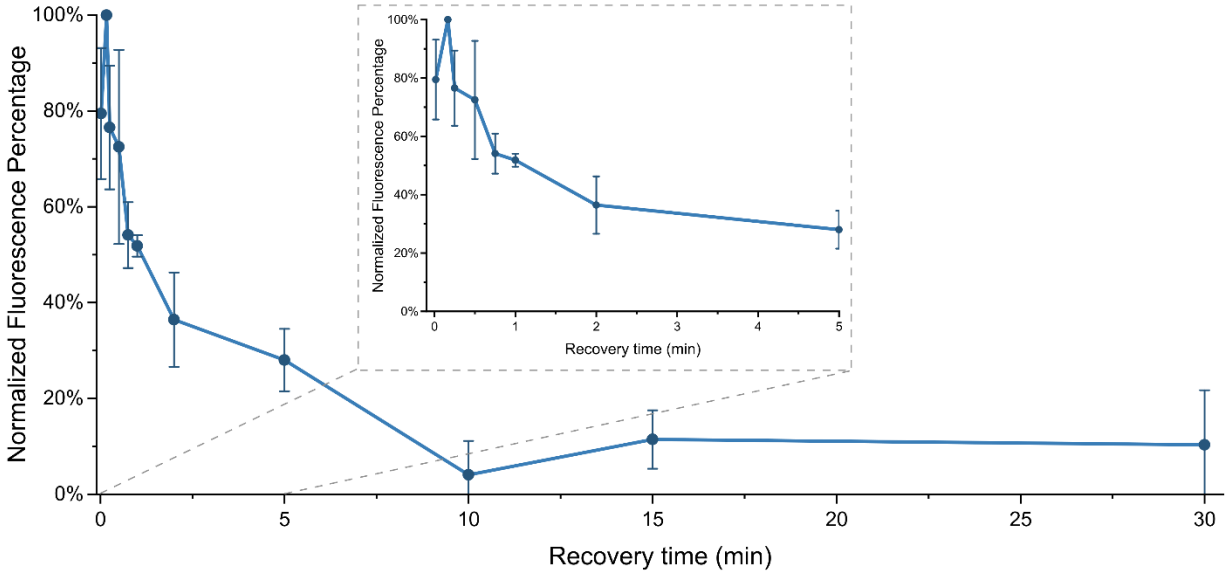

Supplementary Figure 8| C2C12 cell membrane resealing time after NEST treatment, measured by fluorescent 3kDa dextran delivery. Cells were treated with the NEST device, then collected in warm cell culture medium (DMEM + 10% FBS) and allowed to recover for a given time. Then, a small volume of high concentration fluorescent 3kDa dextran was added to the cell solution to a final concentration of 0.1mg/mL. Cells with open membrane pores at the time of dextran addition intake dextran and appear as fluorescent during flow cytometric analysis. Data is normalized so the highest percentage of dextran delivery in each replicate is set to 100% and the lowest is set to 0%. n=3, error bars show standard deviation. **Inset**: enlarged portion of the plot from 0-5 minutes recovery.

Data file (separate file): data sets for the figures shown in the main manuscript.